RIV000117
Submitted: June 29, 2012

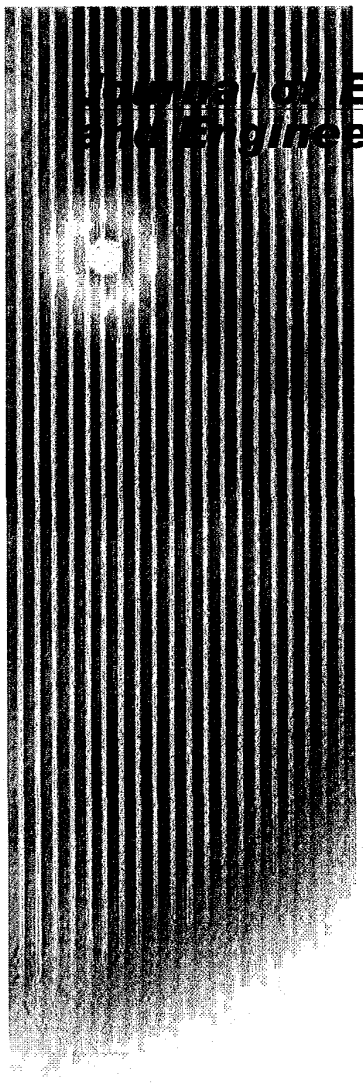

Journal of Environment and Engineering

Development of an Environmental Fatigue Evaluation Method for Nuclear Power Plants in JSME Code*

Makoto HIGUCHI**, Takao NAKAMURA*** and Yasuaki SUGIE****
**IHI Technology Solutions Inc.
1 Shin-nakahara, Isogo-ku, Yokohama, 2358501 Japan
E-mail: makoto_higuchi@ihi.co.jp
***Division of Sustainable Energy and Environmental Engineering, Osaka University
2-1 Yamadaoka, Suita, Osaka, 5650871 Japan
****Codes and Standards Division, Japan Nuclear Technology Institute
4-2-3, Shiba, Minato-ku, Tokyo, 1080014 Japan

Abstract
Many examinations concerning the fatigue life reduction for structural materials of nuclear power plants in simulated LWR coolant have been performed, and the effects of several parameters on fatigue life reduction have been quantified in the time since the first paper on this subject was recognized in Japan. Based on these results, methods to evaluate fatigue damage for materials exposed to LWR coolant have been developed. The MITI Guidelines (2000) and the TENPES Guidelines (2002) were issued for evaluating environmental fatigue damage in operating plants. The Environmental Fatigue Evaluation Method (EFEM) for Nuclear Power Plants (JSME S NF1-2006) was established in the Codes for Nuclear Power Generation Facilities by the JSME by reviewing the equations for the environmental fatigue life correction factor, F_{en}, and the techniques for evaluation based on the most up-to-date knowledge at the time. A revised version of the EFEM was drafted by incorporating updated knowledge and issued by the end of 2009. This paper outlines the revised JSME Codes and technical bases, and discusses the effects of several parameters on fatigue life reduction in such environments.

Key words: Fatigue, Corrosion Fatigue, Nuclear Power Generation, Nuclear Reactor

1. Introduction

Since the first paper[1] was issued regarding the phenomenon that component material fatigue life is reduced in simulated LWR coolant, many studies on this subject have been completed and various factors that can reduce fatigue life have been quantitatively evaluated. The materials covered in the studies include carbon steels, low alloy steels, stainless steels, and nickel chromium iron alloys. Both PWR and BWR environments have been evaluated. Factors tested include strain rate ($\dot{\varepsilon}$ [%/s]), temperature (T [°C]), dissolved oxygen concentrations (DO [ppm]), sulfur contents (S [%]), flow rate (WFR [m/s]), and strain hold time. In addition, tests were performed with fluctuating parameters assuming actual plant transients and the environmental fatigue evaluation method for light water reactors has been developed based on the results of these studies. In September 2000, the Agency for Natural Resources and Energy of the then Ministry of International Trade and Industry (MITI) issued the "Guidelines for Evaluating Fatigue Initiation Life Reduction in the LWR Environment."[2] These guidelines provided only equations to determine fatigue lives in such environments. Accordingly, the Thermal and Nuclear Power Engineering Society (TENPES) issued the "Guidelines on Environmental Fatigue Evaluation for LWR Components"[3] in 2002, which provided the method for applying the environmental fatigue evaluation to operating plants. By reviewing and combining the MITI and TENPES guidelines, the Japan Society of Mechanical Engineers

*Received 7 Dec. 2010 (No. 11-09-0652)
Japanese Original: Trans. Jpn. Soc. Mech. Eng., Vol.76, No.762-A (2010), pp.171-181 (Received 8 July 2009)
[DOI: 10.1299/jee.6.452]

(JSME) established the Environmental Fatigue Evaluation Method (EFEM) for Nuclear Power Plants in its Codes for Nuclear Power Generation Facilities in 2006 (JSME S NF1-2006).[4] A revised version of the EFEM was established by incorporating the most up-to-date information and issued in 2009. This paper summarizes the revised JSME Codes and technical bases concerning the effects of several parameters on fatigue life reduction in LWR environments.

2. Environmental fatigue life correction factor, F_{en}

2.1 Definition of F_{en}

The environmental fatigue life correction factor, F_{en}, is used to evaluate environmental fatigue. F_{en} is defined as the ratio of the fatigue life in air divided by the fatigue life in water at the same strain amplitude, as shown in equation (1).

$$F_{en} = N_A / N_W \tag{1}$$

In equation (1), N_A is the fatigue life in air at room temperature and N_W is the fatigue life in simulated LWR water. N_A can be determined from a reference fatigue curve developed using the least-squares method with data obtained from strain-controlled fatigue tests conducted in Japan. The reference fatigue curves for carbon, low alloy, austenitic stainless steels, and nickel chromium iron alloys can be expressed using the following equations, respectively:

$$\varepsilon_a = 25.71 N_A^{-0.490} + 0.113 \quad \text{(Carbon steel)} \tag{2}$$

$$\varepsilon_a = 38.44 N_A^{-0.562} + 0.155 \quad \text{(Low alloy steel)} \tag{3}$$

$$\varepsilon_a = 23.0 N_A^{-0.457} + 0.11 \quad \text{(Stainless steel)} \tag{4}$$

$$\varepsilon_a = 19.0 N_a^{-0.450} + 0.118 \quad \text{(Ni-Cr-Fe alloy)} \tag{5}$$

2.2 F_{en} for carbon and low alloy steels

2.2.1 Effects of sulfur content

The fatigue life of carbon and low alloy steels in hot water is dependent on the sulfur content within the steels. Figure 1 illustrates the relationship between F_{en} and sulfur content under the condition of 289°C, DO>0.7 ppm, and 0.001%/s strain rate[5]. The plotted points in Figure 1 represent the average F_{en} for various levels of sulfur content in order to eliminate biased trends due to an unbalanced number of data points. Data on weld metals were excluded from the plot because those materials are apparently less sensitive to environmental effects. As shown in Figure 1, the logarithm of F_{en} increases linearly with sulfur content. It was concluded that regarding the effects of sulfur content, there is no significant difference between carbon and low alloy steels, and both data sets were analyzed by a least squares fit.. The resultant line and equation are shown in Figure 1.

2.2.2 Effects of strain increase rate

Figure 2 shows the relationship between F_{en} and strain rate ($\dot{\varepsilon}$) under a 289°C and DO>0.7 ppm environment [5]. To eliminate the effects of different sulfur contents in individual specimens, F_{en} for each specimen was converted to the value of which sulfur content was 0.015% using equation (6).

$$F_{en(S=0.015\%)} = F_{en(S)} / \mathrm{EXP}(97.92 \times (S - 0.015)) \tag{6}$$

The plots represent the average F_{en} for a given strain rate. As the strain rate decreases, $F_{en(S=0.015\%)}$ increases almost linearly in double logarithmic plot. There is little difference between carbon and low alloy steels. The resultant line of a least squares fit and equation are shown in Figure 2.

Figure 3 shows the relationship between F_{en} and strain rate for selected heats including data tested at strain rates below 0.0001%/s[5]. Data for both carbon and low alloy steels are provided for different environments with higher DO (1-8 ppm) and lower DO (0.2 ppm) For both groups of data, F_{en} reaches a threshold at lower strain rates. The strain rate threshold for the group with greater DO is 0.0001%/s, and is 0.0004%/s for the group with a lower DO.

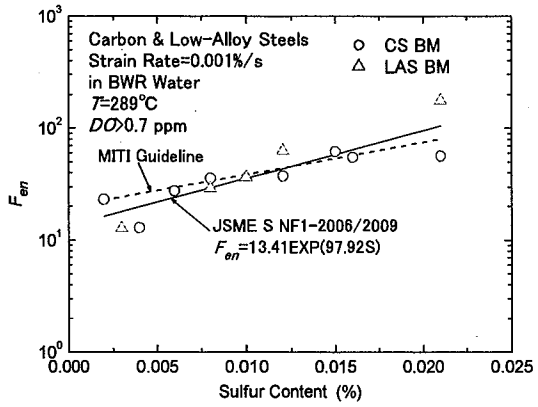

Fig. 1 Relation of sulfur content to F_{en} for carbon and low-alloy steels (average values, excluding weld metals)

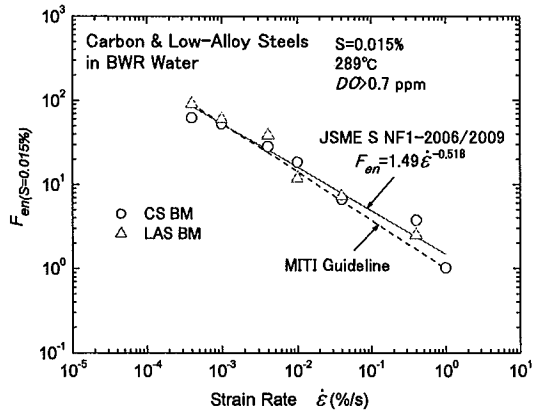

Fig. 2 Relation of strain rate to $F_{en(S=0.015\%)}$ for carbon and low-alloy steels (average values)

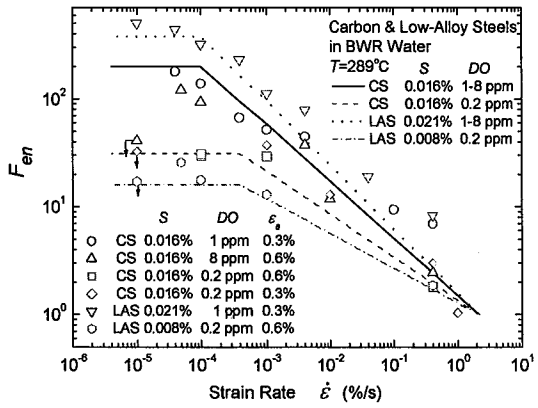

Fig. 3 Relation of strain rate to F_{en} for carbon and low-alloy steels (saturation at low strain rate)

2.2.3 Effects of temperature

Figure 4 shows the relationship between $F_{en(S=0.015\%)}$ and temperature for carbon and low alloy steels under the conditions of DO>0.7 ppm and 0.001%/s strain rate. As shown in the figure, for temperatures between 50 and 160°C, a flat line representing $F_{en(S=0.015\%)}$=6.0 is assumed; for temperatures above 160°C, the relationship is represented by the equation shown in the figure; and for temperatures below 50°C, a line connecting the point (50°C, $F_{en(S=0.015\%)}$=6.0) to the point (0°C, $F_{en(S=0.015\%)}$=1.0) is assumed.

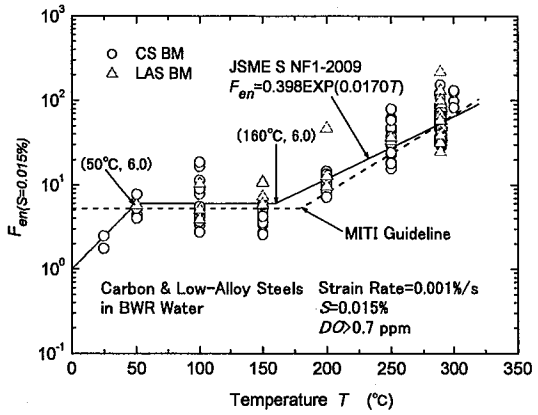

Fig. 4 Relation of temperature to $F_{en(S=0.015\%)}$ for carbon and low-alloy steels

2.2.4 Effects of dissolved oxygen concentration

Figure 5 shows the relationship between $F_{en(S=0.015\%)}$ and dissolved oxygen concentrations for carbon and low alloy steels under the conditions of 289°C and a strain rate of 0.001%/s [5]. The threshold of $F_{en(S=0.015\%)}$ is assumed to be 53.5 at high *DO*, which can be derived by substituting $\dot{\varepsilon} = 0.001\%/s$ in the equation shown in Figure 2. The threshold of $F_{en(S=0.015\%)}$ at low *DO* is assumed to be 3.28, which is derived by averaging the data on carbon and low alloy steels with *DO* of 0.01 ppm or less. A line in the transition zone connecting the point (F_{en}=53.5, *DO*=0.7 ppm) to the point (F_{en}=3.28, *DO*=0.02 ppm) is assumed, as expressed by the equation shown in Figure 5.

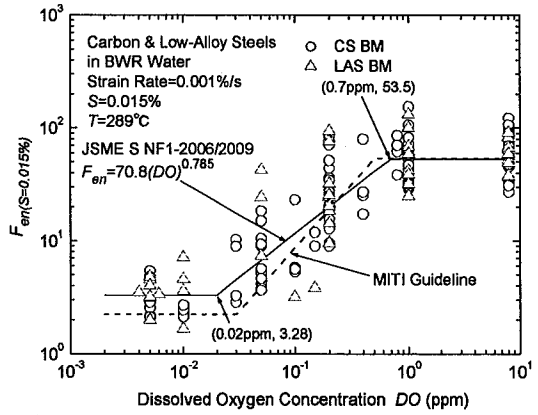

Fig. 5 Relation of *DO* to F_{en} for carbon and low-alloy steels in BWR water

2.2.5 Effects of water flow rate

Figure 6 shows the relationship between F_{en} and water flow rate for carbon steels [5], [6]. F_{en} is highly dependent on the flow rate, under high *DO* and high sulfur content conditions, and decreases as flow rate increases. However, the flow rate has little influence on F_{en} for materials with low sulfur content and/or for environment with low *DO*, in which conditions, F_{en} is essentially small. Accordingly, it can be concluded that the flow rate has no effect on F_{en} in the PWR water and has only a minor influence on F_{en} in BWR feed water, where the *DO* is around 0.05ppm. Similar trends can be seen for low allow steels. The current F_{en} equation, which was formulated based on data taken at lower flow rates, consistently results in a conservative evaluation for high flow rate conditions. Therefore, the effects of flow rate are not considered applicable to carbon and low alloy steels for this evaluation.

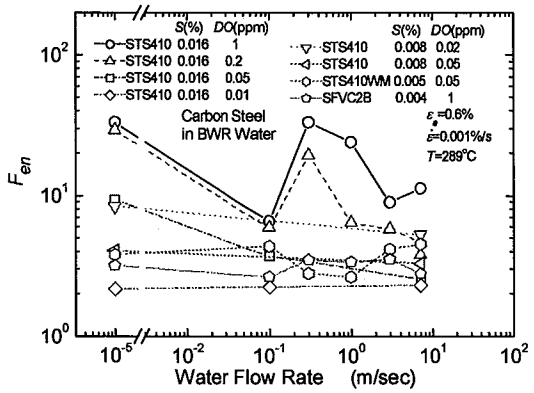

Fig. 6 Relation of water flow rate to F_{en} for carbon steel in BWRs

2.2.6 Effects of material strength

The environmental fatigue tests were also performed for representative high strength materials to be used in the pressure boundary of LWRs, including carbon steel STS480 and low alloy steel SQV2B. The test results confirmed that the environmental effects are not significant for these high strength materials.

2.2.7 Equation to calculate F_{en} for carbon and low alloy steels

An equation to calculate F_{en} for carbon and low alloy steels derived by considering all of the above test results, is shown in Table 1 [5].

Table 1 F_{en} equations for carbon and low alloy steels

$$\ln(F_{en}) = 0.00822(0.772 - \dot{\varepsilon}^*)S^*T^*O^*$$

$\dot{\varepsilon}^* = \ln(2.16)$ $(\dot{\varepsilon} > 2.16\%/s)$

$\dot{\varepsilon}^* = \ln(\dot{\varepsilon})$ $(0.0004 \le \dot{\varepsilon} \le 2.16\%/s, DO \le 0.7\text{ppm})$

$\dot{\varepsilon}^* = \ln(0.0004)$ $(\dot{\varepsilon} < 0.0004\%/s, DO \le 0.7\text{ppm})$

$\dot{\varepsilon}^* = \ln(\dot{\varepsilon})$ $(0.0001 \le \dot{\varepsilon} \le 2.16\%/s, DO > 0.7\text{ppm})$

$\dot{\varepsilon}^* = \ln(0.0001)$ $(\dot{\varepsilon} < 0.0001\%/s, DO > 0.7\text{ppm})$

$S^* = \ln(12.32) + 97.92S$

$T^* = 0.0358T$ $(T < 50°C)$

$T^* = \ln(6)$ $(50 \le T \le 160°C)$

$T^* = \ln(0.398) + 0.017T$ $(T > 160°C)$

$O^* = \ln(3.28)$ $(DO < 0.02\text{ppm})$

$O^* = \ln(70.79) + 0.7853\ln(DO)$ $(0.02 \le DO \le 0.7\text{ppm})$

$O^* = \ln(53.5)$ $(DO > 0.7\text{ppm})$

$F_{en} = 1.0$ ($\varepsilon_a \le 0.042\%$ or in the case of earthquake)

2.3 F_{en} for stainless steels

2.3.1 Effects of strain increase rate

Different equations to calculate F_{en} are applied to BWR and PWR stainless steel components. Figure 7 shows the relationship between F_{en} and strain rate at 289°C in simulated BWR water [5]. Materials are classified into Type 316NG, 304, its associated weld metal, and cast stainless steel, and the average F_{en} values for individual materials are plotted for various strain rates. Data obtained from tests on 316NG, 304 and 304L conducted at high flow rates exceeding 1 m/s are plotted separately. As can be seen in the figure, average F_{en} values for cast steel and those obtained at high flow rates are greater than F_{en} values for non-cast steels tested in stagnant water. It may be possible to apply separate equations to cast steels and non-cast steels. However, due to difficulties in evaluating the data for high flow rates, all of the data are analyzed as a whole using a least squares fit to determine a trend line. The resultant line and equation are shown in Figure 7.

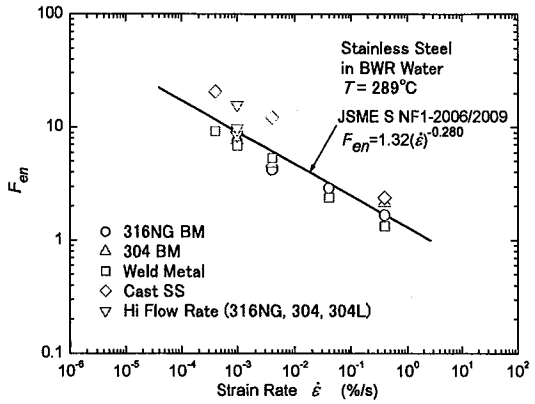

Fig. 7 Relation of strain rate to F_{en} for stainless steel in BWRs

The relationship between F_{en} and strain rate is shown in Figure 8 [5] for 316NG and cast stainless steel (both of for which data are obtained at very low strain rates under a simulated BWR environment at 289°C),. In Figure 8, the trend line described in Figure 7 is also shown. Data for 316NG are not saturated at 0.00004%/s, however this was determined to be the threshold for strain (the same value as for PWRs). This value was chosen since it is closest to the lowest average strain rate at a transient, and even if it is assumed that the strain rate is saturated at 0.00004%/s, it would not significantly influence the result.

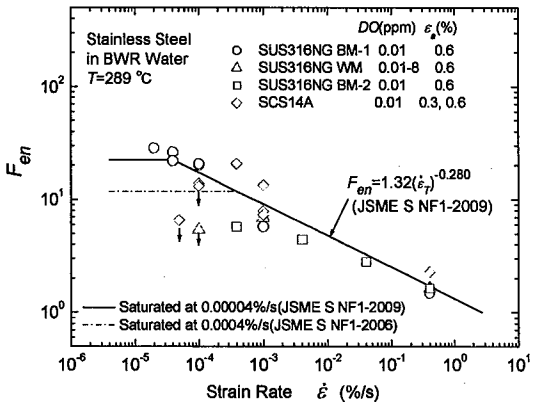

Fig. 8 Relation of strain rate to F_{en} for stainless steel in BWRs (saturation at low strain rate)

Figure 9 shows the relationship between F_{en} and strain rate for stainless steels in a simulated PWR environment at 325°C [5]. Materials are classified into Type 316, 304, its associated weld metal, and cast stainless steel and the average F_{en} values for individual materials at various strain rates are plotted. As shown in this figure, there is no significant difference among the materials, although F_{en} for SUS304 is slightly higher and that for weld metals is slightly lower. Therefore, the data were analyzed as a whole using a least squares fit to determine a trend line. The resultant line and equation are shown in Figure 9.

Figure 10 shows the relationship between F_{en} and strain rate in a simulated PWR environment for cast and non-cast stainless steels for which test data at very low strain rates have been obtained [5]. In Figure10, the trend line in Figure 9 is also shown. As can be seen in the figure, the threshold for lower strain rates for non-cast stainless steel is 0.0004%/s and that for cast stainless steel is 0.00004%/s.

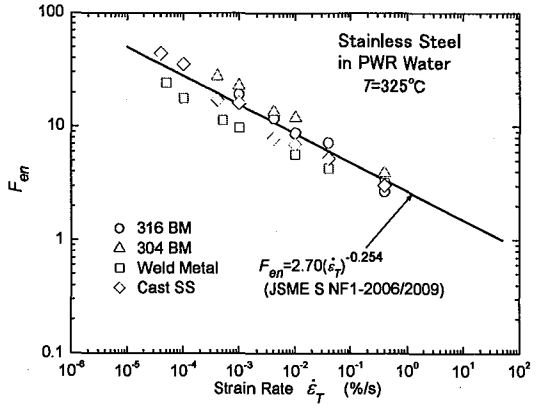

Fig. 9 Relation of strain rate to F_{en} for stainless steel in PWRs

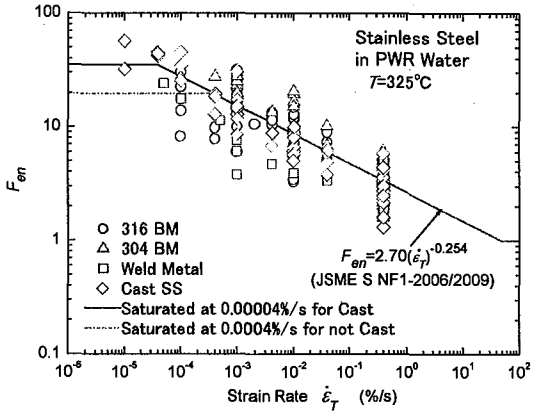

Fig. 10 Relation of strain rate to F_{en} for stainless steel in PWRs (saturation at low strain rate)

2.3.2 Effects of temperature

The relationship between F_{en} and temperature in a simulated BWR environment is shown in Figure 11 [5]. The trend line in Figure 11 was not obtained using a least squares fit of the data, but was derived by connecting the F_{en} value (9.14), which was obtained by substituting $\dot{\varepsilon} = 0.001\%/s$ into the BWR trend line at 289°C (shown in Figure 7) to the point, F_{en} =1 at 0°C. The equation for the trend line is shown in Figure 11.

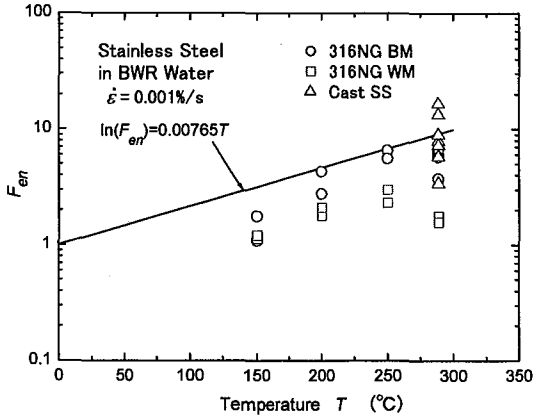

Fig. 11 Relation of temperature to F_{en} for stainless steel in BWRs

Figure 12 shows the relationship between F_{en} and temperature in a simulated PWR environment[5]. The trend line in Figure 12 is derived by connecting the F_{en} value (14.76), which was obtained by substituting $\dot{\varepsilon} = 0.001\%/s$ into the PWR trend line at 325°C (shown in Figure 9) to the point, F_{en}=1 at 0°C. The equation for the trend line is shown in Figure 12.

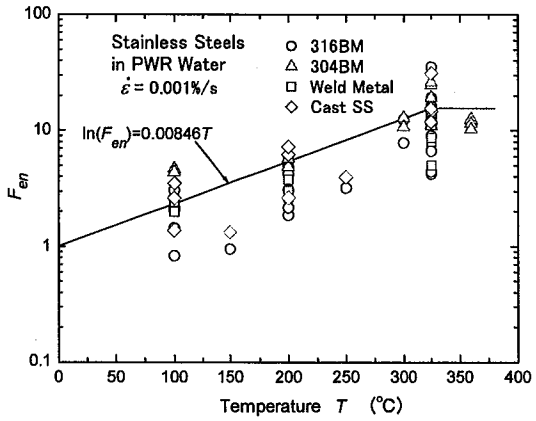

Fig. 12 Relation of temperature to F_{en} for stainless steel in PWRs

2.3.3 Effects of dissolved oxygen concentration

The effect of dissolved oxygen concentration on F_{en} for stainless steels was not clearly seen in either the simulated BWR or PWR environments. Accordingly, it is concluded that the effect of dissolved oxygen concentration on stainless steels is negligible in this evaluation.

2.3.4 Effects of water flow rate

Figure 13 shows the relationship between F_{en} and water flow rate in the simulated BWR environment for three types of stainless steels[5, 6]. Contrary to carbon steels, F_{en} for stainless steels becomes larger at higher flow rates (indicating that the life of stainless steel decreases under higher flow rates). The extent of increase in F_{en} at high flow rates depends on the material with the largest increase being for SUS304. With a large dispersion in the data it is impossible to quantify a dependency on the flow rate. Therefore, as described in the above section 2.3.1 "Effects of strain increase rate", three averaged F_{en} values at a strain rate of 0.001%/s and a high flow rate exceeding 1m/s for the three types of stainless steels are incorporated into the data set. This is used to determine the relationship between F_{en} and strain rate.

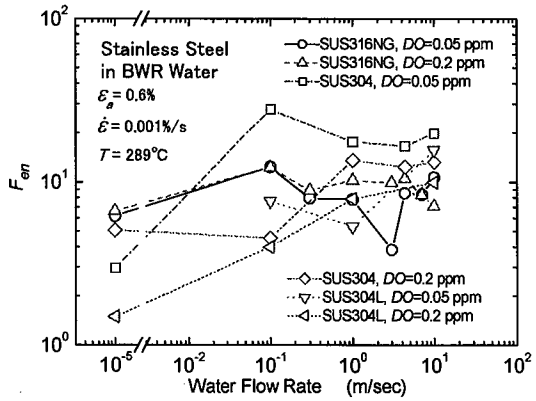

Fig. 13 Relation of water flow rate to F_{en} for stainless steel in BWRs

As shown in Figure 14, F_{en} is not dependent on the flow rate in the PWR environment[5].

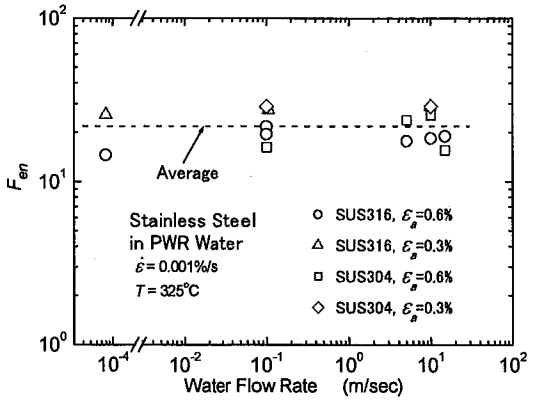

Fig. 14 Relation of water flow rate to F_{en} for stainless steel in PWRs

2.3.5 Effects of sensitization

There is no significant difference in F_{en} between sensitized and solution-treated SUS304 base metal in the simulated BWR environment, and thus it is concluded that the sensitization has no effect on F_{en} in the BWR environment. In addition, the results of many fatigue tests for thermally-aged materials have shown that there is not a significant dependence of thermal ageing on the fatigue life for most of the tested materials.

2.3.6 Equation to calculate F_{en} for stainless steels

An equation to calculate F_{en} for stainless steels derived considering the above test results, is shown in Table 2 [5].

Table 2 F_{en} equations for austenitic stainless steels

$\ln(F_{en}) = (C - \dot{\varepsilon}^*)T^*$
C=0.992 (BWR)
C=3.910 (PWR)
$\dot{\varepsilon}^* = \ln(2.69)$ (BWR : $\dot{\varepsilon} > 2.69\%/s$)
$\dot{\varepsilon}^* = \ln(49.9)$ (PWR : $\dot{\varepsilon} > 49.9\%/s$)
$\dot{\varepsilon}^* = \ln(\dot{\varepsilon})$ (BWR : $0.00004 \le \dot{\varepsilon} \le 2.69\%/s$)
(PWR not Cast : $0.0004 \le \dot{\varepsilon} \le 49.9\%/s$)
(PWR Cast : $0.00004 \le \dot{\varepsilon} \le 49.9\%/s$)
$\dot{\varepsilon}^* = \ln(0.0004)$ (PWR not Cast : $\dot{\varepsilon} < 0.0004\%/s$)
$\dot{\varepsilon}^* = \ln(0.00004)$ (BWR, PWR Cast : $\dot{\varepsilon} < 0.00004\%/s$)
$T^* = 0.000969T$ (BWR)
$T^* = 0.000782T$ (PWR: $T \le 325$°C)
$T^* = 0.254$ (PWR: $T > 325$°C)
F_{en} =1.0 ($\varepsilon_a \le 0.11\%$ or in the case of earthquake)

2.4 F_{en} for nickel chromium iron alloy

2.4.1 Effects of strain increase rate

For nickel chromium iron alloys it is necessary to adopt different F_{en} equations for the BWR and PWR environments. Figure 15 shows the relationship between F_{en} and strain rate for nickel chromium iron alloy in a simulated BWR environment at 289°C [5]. The data for Alloy 600 conventional, Alloy 600 modified with higher SCC resistance, and type 182 weld metal are plotted separately in this figure. Since no clear differences were observed in the behavior of these materials, it was determined that the data could again be analyzed as a whole. Although there is relatively large scatter in the data, the line and equation shown in the figure were derived using a least squares fit. The slope of this line is significantly less than that for other materials, which suggests that the fatigue life of nickel chromium iron alloy is less sensitive to the BWR environment.

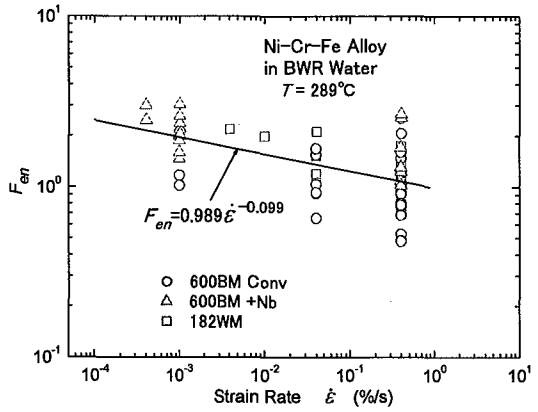

Fig. 15 Relation of strain rate to F_{en} for Ni-Cr-Fe alloys in BWRs

Figure 16 shows the relationship between F_{en} and strain rate for nickel chromium iron alloys in a simulated PWR environment[5]. The data for Alloy 600 base metal, type 132 weld metal, Alloy 690 base metal and type 152 weld metal are plotted separately in the figure. Both Alloy 600 and Alloy 690 are less sensitive to the PWR environment, although there is a slight difference between these materials. It was determined that the data could be analyzed as a single sample set. The line and equation shown in Figure 16 were obtained by analyzing all test data using a least squares fit. The threshold for lower strain rates was set at 0.00004%/s for BWRs and 0.0004%/s for PWRs respectively–similar to those of rolled stainless steel since the amount of data was insufficient to perform the analysis.

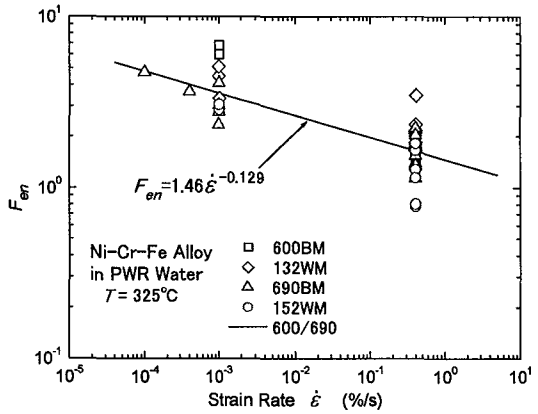

Fig. 16 Relation of strain rate to F_{en} for Ni-Cr-Fe alloys in PWRs

2.4.2 Effects of temperature

Figure 17 shows the relationship between F_{en} and temperature for nickel chromium iron alloys in LWR water at a strain rate of 0.001%/s[5]. Since a limited amount of data was obtained from fatigue tests at different temperatures, it is difficult to identify the relationship between F_{en} and temperature. Therefore, a logarithmic linear relationship between F_{en} and temperature is assumed (similar to stainless steels), and straight lines connecting the average F_{en} values at 289°C for BWRs and at 325°C for PWRs to the point (0°C, F_{en}=1.0) are plotted. The figure also shows the relationship between F_{en} and temperature for austenitic stainless steel in simulated PWR and BWR environments.

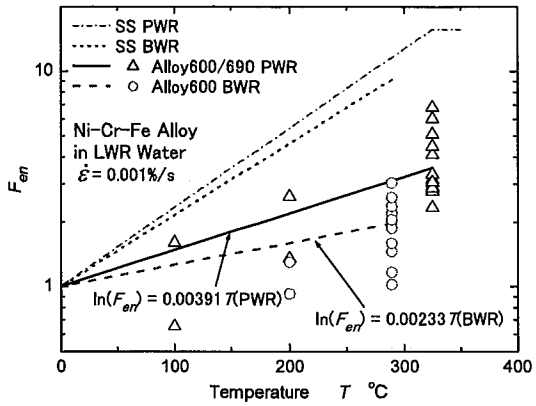

Fig. 17 Relation of temperature to F_{en} for Ni-Cr-Fe alloys in LWR water

2.4.3 Effects of dissolved oxygen concentration

It has been confirmed that F_{en} for nickel chromium iron alloys does not depend on the dissolved oxygen concentration.

2.4.4 Equation to calculate F_{en} for nickel chromium iron alloys

An equation to calculate F_{en} for nickel chromium iron alloys, derived considering the above test results, is shown in Table 3 [5].

Table 3 F_{en} equations for Ni-Cr-Fe alloys

$\ln(F_{en}) = (C - \dot{\varepsilon}^*)T^*$
C=0.112 (BWR)
C=2.94 (PWR)
$\dot{\varepsilon}^* = \ln(0.894)$ (BWR : $\dot{\varepsilon} > 0.894\%/s$)
$\dot{\varepsilon}^* = \ln(19.0)$ (PWR : $\dot{\varepsilon} > 19.0\%/s$)
$\dot{\varepsilon}^* = \ln(\dot{\varepsilon})$ (BWR : $0.00004 \le \dot{\varepsilon} \le 0.894\%/s$)
(PWR : $0.0004 \le \dot{\varepsilon} \le 19.0\%/s$)
$\dot{\varepsilon}^* = \ln(0.00004)$ (BWR : $\dot{\varepsilon} < 0.00004\%/s$)
$\dot{\varepsilon}^* = \ln(0.0004)$ (PWR : $\dot{\varepsilon} < 0.0004\%/s$)
$T^* = 0.000343T$ (BWR)
$T^* = 0.000397T$ (PWR)
F_{en} =1.0 ($\varepsilon_a \le 0.11\%$ or in the case of earthquake)

3. Evaluation of F_{en} during actual transients

3.1 Evaluation of F_{en} under inconsistent conditions

The equations to calculate F_{en} are provided assuming consistent conditions are maintained. However, under an actual transient strain rates and temperatures fluctuate. F_{en} may be calculated for a fatigue test by increasing strain rates in a stepwise manner, as shown in Figure 18, by using an F_{en} equation used in the constant strain rate test according to one of the following three models (F_{encal}):

(1) Mean strain rate model

(2) Time-based integral model

F_{en} weighted with the loading time is integrated. The method, which was proposed by Mehta [8], can be expressed by Equation (7) shown below:

$$F_{en,tbi} = (1/t_{T,th}) \int_0^{T,th} \{F_{en}(t)\} dt \quad (7)$$

(3) Strain-based integral model

F_{en} for individual strain rates weighted with strain gains is integrated. The method, which was proposed by Kishida et al.[9] and Higuchi et al.[10] can be expressed by Equation (8) shown below. This is called the modified rate approach.

$$F_{en,mra} = \int_{\varepsilon_{min}}^{\varepsilon_{max}} \{F_{en}(\varepsilon')/\varepsilon_{max} - \varepsilon_{min})\} d\varepsilon \quad (8)$$

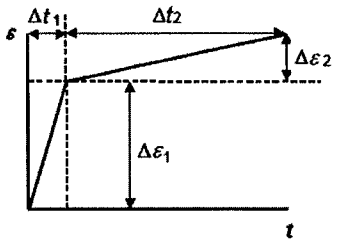

Fig. 18 A sample of strain wave for a 2-step strain rate change fatigue test

Calculated results are compared with F_{entest} for carbon steels in a simulated BWR environment in Figure 19 [7].

The results calculated using the time-based integral model show few variations, even under different conditions. In particular, the calculated results in the range with small strain changes at lower strain rates are excessively conservative. The strain-based integral model shows the best correlation with the test results. The results calculated by the mean strain rate model are located between those calculated using the strain-based or time-based methods. Considering these results, the modified rate approach is suitable for calculating F_{en}, and the mean strain rate model enables a simplified evaluation and provides conservative results. Similar results have been observed for stainless steels. During a transient at an actual plant, temperatures, dissolved oxygen concentration, and strain rate may change. Several fatigue tests have been conducted in simulated BWR and PWR environments while changing temperatures, strain rates and other conditions [11, 12]. Considering the results of these tests, it is concluded that the modified rate approach is suitable for evaluating F_{en} under any conditions.

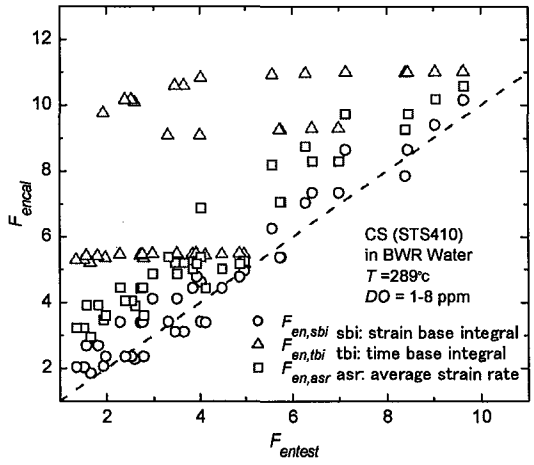

Fig. 19 Comparison of $F_{en,sbi}$, $F_{en,tbi}$ and $F_{en,asr}$ for carbon steel in BWRs

3.2 Evaluation of F_{en} considering the effects of strain holding

In the BWR environment, the fatigue life of materials is reduced due to strain holding at the peak stress intensity (local maximum value) [13]. The relationship between F_{en} and strain hold time is shown for carbon steels, low alloy steels, and stainless steels in Figures 20-22,

respectively. In these figures, the test results under the strain holding at the peak, peak minus 0.03% and peak minus 0.06% are also shown.

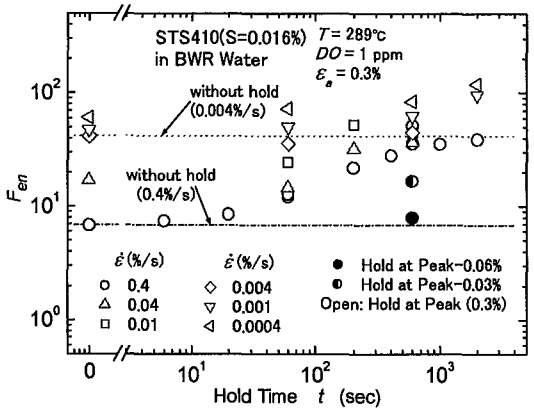

Fig. 20 Relation of hold time to F_{en} for carbon steel in BWRs

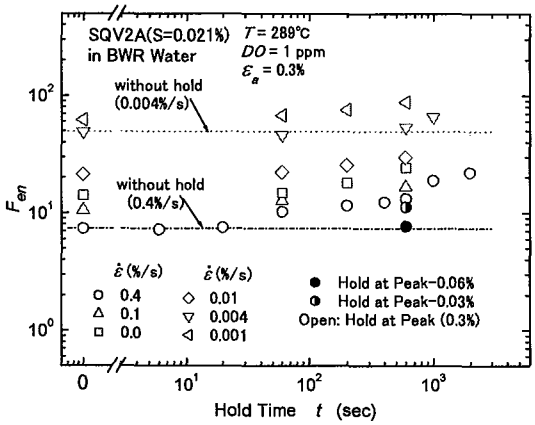

Fig. 21 Relation of hold time to F_{en} for low alloy steel in BWRs

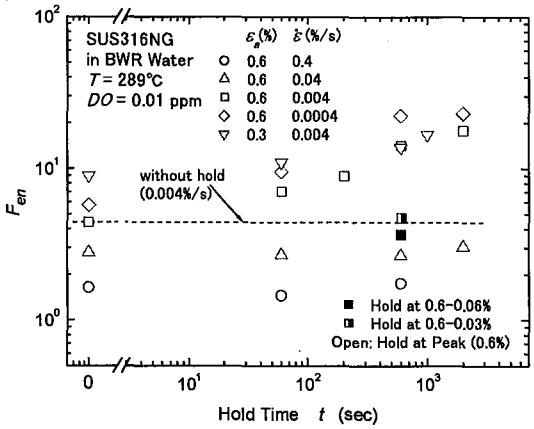

Fig. 22 Relation of hold time to F_{en} for stainless steel in BWRs

On the plots for carbon and low alloy steels, the dotted lines represents F_{en} at a strain rate of 0.004%/s without holding, and the dotted and dashed lines represents F_{en} at a strain rate of 0.4%/s without holding. On the plot for stainless steels, the dotted line represents F_{en} at a strain rate of 0.004%/s without holding. In each case, F_{en} increases due to strain holding at the peak. For carbon and low alloy steels, fatigue life reduction becomes negligible at a strain rate of

0.004%/s or lower. Conversely, fatigue life reduction is significant for stainless steels even at lower strain rates, and does not become saturated as the strain holding time becomes longer.

When the strain rate is maintained slightly below the peak and thermal transients are taken into account, no fatigue life reduction is observed even though tensile stresses corresponding to the yield point remain. It can be concluded that under normal thermal transient conditions, it is not necessary to consider fatigue life reduction due to strain holding. Considering the above results, it was determined that for calculating the reduction in fatigue life due to strain holding, if the peak stress intensity to be used in the fatigue life evaluation is equal to that during operation at rated power output and the strain increases to a peak value and then is retained, the strain rate shall be treated as follows:

- Carbon and low alloy steels: Strain rates above 0.004%/s are treated as a strain rate of 0.004%/s/
- Stainless steels: The strain rate is set at 0.00004%/s.
- Nickel chromium iron alloys: Reduction in fatigue life due to strain holding is not considered.

No fatigue life reduction due to strain holding was observed under a PWR environment, as shown in Figure 23 [13].

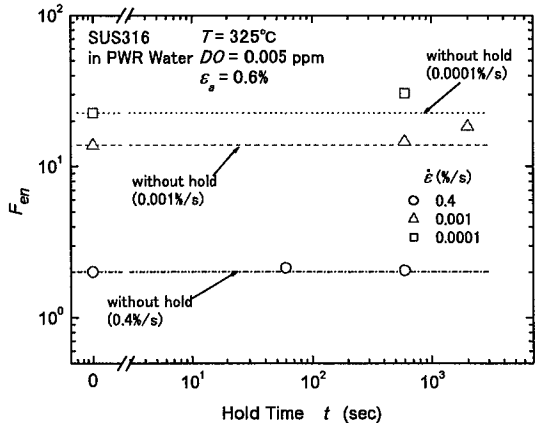

Fig. 23 Relation of hold time to F_{en} for stainless steel in PWRs

4. Codes for Nuclear Power Generation Facilities – Environmental Fatigue Evaluation Method for Nuclear Power Plants-

4.1 General

The Codes specify a fatigue evaluation method that accounts for the influence of environmental effects found in structures exposed to light water reactor cooling water, including PWR secondary system water. The Codes apply to materials such as carbon steels, low allow steels, austenitic stainless steels and nickel chromium iron alloys, which are used for light water reactors (and are authorized for use by the JSME Rules on Materials for Nuclear Facilities (JSME S NJ1-2008)) . The Codes are applicable to a range of temperature and water chemistry conditions consistent with LWR design and operating conditions. The Codes do not specifically mention at which stage they should be applied (i.e., plant design, construction or maintenance).

4.2 Methods to evaluate environmental effects

Cumulative fatigue usage factors in the air are calculated using the methods specified in existing Codes. The cumulative fatigue usage factor in the environment, U_{en}, is expressed by Equation (9) below:

$$U_{en} = U \times F_{en} = \sum_{i=1}^{n} U_i \times F_{en,i} \qquad (9)$$

In Equation (9), U_i refers to the cumulative fatigue usage factor in the i[th] stress cycle out of n total cycles; and $F_{en,i}$ is F_{en} during the i[th] stress cycle and is determined for individual materials as a function of strain rate, temperature, dissolved oxygen concentration and other parameters.

It is known that environmental effects disappear at small strain amplitudes [1, 5]. Based on this understanding, the threshold of strain amplitude is set at 0.042% for carbon steels, which is equal to the strain amplitude at 10^6 cycles in the current design fatigue curve. Similarly, the threshold is set at 0.11% for stainless steels and nickel chromium iron alloys, which is equal to the strain amplitude at the fatigue limit. Below these values, environmental effects need not be considered.

Environmental effects disappear at high strain rates, as mentioned in the section regarding the effects of strain rate. Fatigue evaluation of thermal transient events is normally required to consider environmental effects because strain rates are low during such events. However, seismic loading cycles are excluded from the environmental fatigue evaluation because seismic load cycles are characterized by high strain rates of short duration.

4.3 Method to calculate environmental fatigue correction factor F_{en}

To calculate F_{en}, the range in which strain during a transient increases in a continuous manner is divided into several time segments, and calculations are performed for each segment. Three methods to determine F_{en}, are available:

(1) Factor multiplication method

The factor multiplication method performs the evaluation in the simplest and most conservative manner according to the design conditions of the location subject to the evaluation. In the calculation, the lower threshold of strain rate, maximum service temperature of the concerned location and expected maximum dissolved oxygen concentration are used.

(2) Simplified method

To perform an evaluation using the simplified method, $F_{en,simp,A}$ and $F_{en,simp,B}$ are calculated respectively for two transients (A and B), which constitute the stress cycle used in the calculation of a fatigue usage factor. As shown in Figure 24, the time segments evaluated for each transient are those where strain is increasing the ($\varepsilon_{min} \rightarrow \varepsilon_{max}$) . . After defining the strain rate, average strain rate, maximum service temperature and maximum dissolved oxygen concentration in these segments, $F_{en,simp,A}$ and $F_{en,simp,B}$ are calculated.

$F_{en,simp}$ of a stress cycle is calculated using Equation (10), below. The larger of $F_{en,simp,A}$ and $F_{en,simp,B}$, is used in the equation.

$$F_{en,simp} = \frac{F_{en,simp,A} \times (\varepsilon_{\max,A} - \varepsilon_{\min,A}) + F_{en,sim,B} \times (\varepsilon_{\max,B} - \varepsilon_{\min,B})}{(\varepsilon_{\max,A} - \varepsilon_{\min,A}) + (\varepsilon_{\max,B} - \varepsilon_{\min,B})} \quad (10)$$

(3) Detailed method

To perform an evaluation using the detailed method, $F_{en,simp,A}$ and $F_{en,simp,B}$ are calculated for two transients (A and B), which constitute the stress cycle used in the calculation of a fatigue usage factor.. As shown in Figure 24, the range where strains continuously increase ($\varepsilon_{min} \rightarrow \varepsilon_{max}$) are divided into m-number segments to be evaluated.. The average strain rate, maximum metal temperature at the wetted section, and maximum dissolved oxygen concentration for each segment are used to calculate $F_{en,simp,A}$ and $F_{en,simp,B}$. $F_{en,det}$ during each transient is calculated using Equation (11) below:

$$F_{en,det} = \sum_{k=1}^{m} F_{en,k} \frac{\Delta\varepsilon_k}{\varepsilon_{\max} - \varepsilon_{\min}} \quad (11)$$

Although the detailed method is most complicated to calculate F_{en}, it can reduce excessive conservativeness.

The Codes specify different evaluation methods for vessels, pipes, pumps, valves and core internals. The largest difference between the evaluation methods among the components is the methods used to calculate strain rates. If the stress analysis according to time histories is

performed, strain rates are calculated from the results of the stress analysis. If not, as in the case for pipes, strain rates are calculated according to the following procedure:

First, the bending moment term (M) and the temperature difference terms (ΔT_1, ΔT_2, and $T_a - T_b$) of Equation (12) are evaluated to determine which is dominant. If the M term is dominant, the strain rate is assumed to be equal to the linearized strain rate of the "startup" transient. If one of the temperature difference terms (ΔT_1, ΔT_2, or $T_a - T_b$) is dominant, the strain rate is obtained based on the assumption that the strains increase linearly from the minimum to the maximum value. In this case, these minimum and maximum strain values are of the most dominant term among the terms ΔT_1, ΔT_2, and $T_a - T_b$ for the transient being evaluated.

$$S_p = \underbrace{\frac{K_1 C_1 P_0 D_0}{2t}}_{P} + \underbrace{\frac{K_2 C_2 M_{is}}{Z_i}}_{M} + \underbrace{\frac{K_3 E\alpha|\Delta T_1|}{1.4}}_{\Delta T_1} + \underbrace{K_3 C_3 E_{ab}|\alpha_a T_a - \alpha_b T_b|}_{T_a - T_b} + \underbrace{\frac{E\alpha|\Delta T_2|}{0.7}}_{\Delta T_2} \quad (12)$$

Refer to the article PPB-3532 in the Rules on Design and Construction for Nuclear Power Plants (JSME S NC1) [14] for the definitions of symbols in Equation (12).

5. Conclusion

In its 2006 Codes for Nuclear Power Generation Facilities (JSME S NF1) in 2006, the Japan Society of Mechanical Engineers (JSME) established an Environmental Fatigue Evaluation Method (EFEM) for Nuclear Power Plants describing the methods to evaluate fatigue life of components in contact with LWR cooling water. In 2009, the JSME S NF1 Codes were revised. This paper presents an outline of the Codes and their technical basis.

- The environmental fatigue life correction factor F_{en} is used in the evaluation of environmental fatigue, F_{en} is determined for individual materials as a function of different factors.
- The Codes specify three types of evaluation methods: the factor multiplication method, the simplified method, and the detailed method. Any of these methods may be selected for use arbitrarily. In addition, conditions which do not require the consideration of environmental effects are specified.
- For carbon and low alloy steels, F_{en} is defined in as a function of strain rate, temperature, dissolved oxygen concentration and sulfur content.
- For stainless steels and nickel chromium iron alloys, F_{en} is defined in as a function of strain rate and temperature.
- The modified rate approach method is specified to evaluate environmental effects under conditions of changing strain rates, temperatures and dissolved oxygen concentrations.
- A reduction of fatigue life due to high water flow rates is considered for stainless steels in a BWR environment.
- A reduction of fatigue life due to strain holding is considered for carbon steels, low alloy steels and stainless steels in a BWR environment.

References

(1) Higuchi, M. and Iida, K., "Fatigue Strength Correction Factors for Carbon and Low-Alloy Steels in Oxygen-Containing High-Temperature Water", *Nuclear Engineering and Design* Vol. 129 (1991), pp. 293-306

(2) "Guidelines for Evaluating Fatigue Life Reduction in the LWR Environment", (in Japanese), Nuclear and Safety Management Division, Agency for Natural Resources and Energy (2000)

(3) "Guidelines on Environmental Fatigue Evaluation for Power Reactors", Thermal and Nuclear Power Engineering Society (2002)

(4) Code for Nuclear Power Generation Facilities, Environmental Fatigue Evaluation Method for Nuclear Power Plants (JSME S NF1-2006), Japan Society of Mechanical Engineers (2006)

(5) Sakaguchi, K., Higuchi, M., Hirano, A., and Nomura, Y., "Final Proposal of Environmental Fatigue Life Correction Factor (F_{en}) for Structural Materials in LWR Water Environments", American

Society of Mechanical Engineers, Pressure Vessel and Piping Conference (ASME PVP) -07-26100, (2007)

(6) Hirano, A., Sakaguchi K., and Shoji, T., "Effects of Water Flow Rate on Fatigue Life of Structural Steels under Simulated BWR Environment", ASME PVP -07-26423, (2007)

(7) Higuchi, M., Hirano, T. and Sakaguchi, K., "Evaluation of fatigue damage on operating plant components in LWR water", ASME PVP2004-2684,.(2004)

(8) Mehta, H. S., "An Update on The EPRI/GE Environmental Fatigue Evaluation Methodology and Its Applications", ASME PVP Vol. 386, pp.183-193., (1999)

(9) Kishida, K., Umakoshi, T. and Asada, Y., "Advances in Environmental Fatigue Evaluation for Light Water Reactor Components", American Society of Testing and Materials, Special Technical Publications (ASTM STP) 1298, p. 282., (1997)

(10) Higuchi, M., Iida, K. and Asada, Y., "Effects of Strain Rate Change on Fatigue Life of Carbon Steel in High-Temperature Water", ASTM STP 1298, pp. 216-231, (1997).

(11) Hirano, A. and Sakaguchi, K., "Modified rate approach method to evaluate fatigue life of carbon steel under simulated synchronously changing BWR conditions", ASME PVP2006- 94006, (2006)

(12) Sakaguchi, K., Nomura, Y., Suzuki, S. and Kanasaki, H., "Applicability of the Modified Rate Approach Method Under Various Conditions Simulating Actual Plant Conditions", ASME PVP2006-93220., (2006)

(13) Higuchi, M., Sakaguchi, K., and Nomura, Y., "Effects of Strain Holding and Continuously Changing Strain Rate on Fatigue Life Reduction of Structural Materials in Simulated LWR Water", ASME PVP-07-26101, (2007)

(14) Code for Nuclear Power Generation Facilities, Rules on Design and Construction for Nuclear Power Plants (JSME S NC1-2008), Japan Society of Mechanical Engineers (2008)